Inorganic Chemistry

Communication

pubs.acs.org/IC

Chiral Single-Chain Magnet: Helically Stacked [$Mn^{III}_2Cu^{II}$] Triangles

Takuya Shiga,[†] Kazuya Maruyama,[†] Graham N. Newton,[†] Ross Inglis,[‡] Euan K. Brechin,*[,‡] and Hiroki Oshio*[,†]

[†]Graduate School of Pure and Applied Sciences, University of Tsukuba, Tennodai 1-1-1, Tsukuba, Ibaraki 305-8571, Japan

[‡]EaStCHEM School of Chemistry, University of Edinburgh, West Mains Road, Edinburgh EH9 3JJ, U.K.

Supporting Information

ABSTRACT: The one-dimensional complex $[Mn^{III}_2Cu^{II}(\mu_3\text{-}O)(Cl\text{-}sao)_3(EtOH)_2]\cdot EtOH$ (Mn_2Cu) was obtained by the metal replacement reaction of the trinuclear manganese complex $(Et_3NH)[Mn^{III}_3(\mu_3\text{-}O)Cl_2(Cl\text{-}sao)_3(MeOH)_2(H_2O)_2]$ with $[Cu(acac)_2]$. The Mn_2Cu chain exhibits single-chain-magnet behavior with finite-size effects due to its large magnetic anisotropy.

Chiral compounds are an important class of materials that attract research interest from the viewpoints of asymmetric catalysis, nonlinear optics, and ferroelectrics.[1] The combination of magnetism and chirality in a molecular system can permit access to properties with applications in magnetooptical devices such as magnetochiral dichromism[2] and chiral magnetostructural effects,[3] as exemplified by the first molecule-based chiral magnet, $[Z^{II}(bpy)_3]_n[M^{II}M^{III}(ox)_3]$ (Z = Ru, Fe, Co, Ni, Zn; M^{II} = Mn, Fe, Co, Cu; M^{III} = Cr, Fe), reported by Coronado and co-workers in 2001.[3f] In contrast to bulk magnets, which are magnetized below a critical temperature and act as permanent magnets, single-molecule magnets (SMMs)[4] and single-chain magnets (SCMs) are nanomagnets, which show slow relaxation of the magnetization due to the activation barrier of magnetic domain reorientation. Since the discovery of SMMs and SCMs, the processes associated with the reorientation of magnetic domains have been extensively studied.[5]

The synergy between quantum magnetism and chirality is attracting intense research interest. Dielectric relaxation was observed in a chiral trinuclear SMM, $[Mn^{III}_3O(Meppz)_3(EtOH)_4(OAc)]$ [Meppz = 3-(5-methyl-2-phenolate)pyrazolate)],[6] and second-harmonic generation (SHG) was confirmed in the chiral SCM complex $[Co(hfac)_2(NITPhOMe)]$ (NITPhOMe = 4′-methoxymethyl-4,4,5,5-tetramethylimidazoline-1-oxyl 3-oxide).[7] Single crystals of molecular species with nonsymmetric structures can be obtained either by use of optically active ligands or by spontaneous resolution during crystallization. Previously, we found that multinuclear Mn^{III} complexes undergo substitution reactions with Cu^{II} ions to form heterometallic complexes,[8] while salicylaldoxime-based ligands have proven to support a diverse range of molecular magnets.[9] During the course of our research, we found that the reaction of the SMM $(Et_3NH)[Mn^{III}_3(\mu_3\text{-}O)Cl_2(Cl\text{-}sao)_3(MeOH)_2(H_2O)_2]$[10] (**1**; H_2Cl-sao = 5-chlorosalicylaldoxime) with $[Cu(acac)_2]$ yielded the chiral cluster $[Mn^{III}_2Cu^{II}(\mu_3\text{-}O)(Cl\text{-}sao)_3(EtOH)_2]\cdot EtOH$ (**2**) where the complex units stack to form a chiral SCM. Herein we report the synthesis and magnetic properties of this heterometallic, chiral SCM.

The reaction of **1** with $[Cu(acac)_2]$[11] in ethanol gave the heterometal complex **2** (Figure 1a) as brown needles.[12]

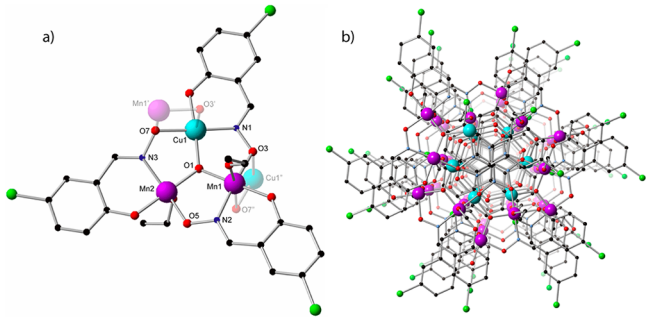

Figure 1. (a) The molecular structure of the asymmetric unit of **2**. (b) One-dimensional structure viewed along the *c* axis. Selected bond lengths (Å): Cu1−N1 1.894(6), Cu1−O1 1.911(7), Cu1−O2 1.894(6), Cu1−O7 1.899(7), Cu1−O3′ 2.642(8), Mn1−N2 1.970(8), Mn1−O1 1.828(7), Mn1−O3 1.879(7), Mn1−O4 1.869(7), Mn1−O8 2.207(12), Mn1−O7′′ 2.448(8), Mn2−N3 1.997(8), Mn2−O1 1.843(7), Mn2−O5 1.904(7), Mn2−O6 1.838(7), Mn2−O9 2.140(9). Color code: manganese, purple; copper, light blue; carbon, black; nitrogen, blue; oxygen, red; chlorine, green. Hydrogen atoms and lattice solvent molecules have been omitted for clarity.

Elemental analysis confirmed that **2** contains one copper and two manganese ions. **2** crystallizes in the enantiomeric hexagonal space groups $P6_1$ and $P6_5$, and structural analyses conducted on several samples suggested that **2** was isolated as a 1:1 mixture of $P6_1$ and $P6_5$ enantiomers. Assignments of the metal ions and their oxidation states were performed based on charge balance considerations and bond-valence-sum (BVS) calculations.[13] In **2**, three metal ions are bridged by a $\mu_3\text{-}O^{2-}$ ion to form a heteronuclear triangle, and the trinuclear units stack to form a helical structure. The coordination geometries of Cu1 and Mn2 are square-pyramidal, while Mn1 has an elongated octahedral coordination environment. The Jahn−Teller elongation axes of all metal ions lie perpendicular to the triangular plane, while their equatorial sites are occupied by one nitrogen and three oxygen atoms from the $\mu_3\text{-}O^{2-}$ and Cl-sao^{2-} ions. Ethanol molecules occupy apical positions on both manganese centers, while the coordination environments of Cu1 and Mn1 are completed by

Received: January 30, 2014
Published: April 17, 2014

   dx.doi.org/10.1021/ic5002418 | *Inorg. Chem.* 2014, 53, 4272−4274

the oxygen atoms (O3* and O7*, respectively) of the aldoxime groups in the neighboring unit. As a result, the triangles stack to form chiral helices (Figure 1b).

Magnetic susceptibility measurements on a powdered sample of **2** were performed in the temperature range 0.5−300 K (Figure 2). The $\chi_m T$ value at 300 K of 4.55 emu mol^{-1} K is smaller than

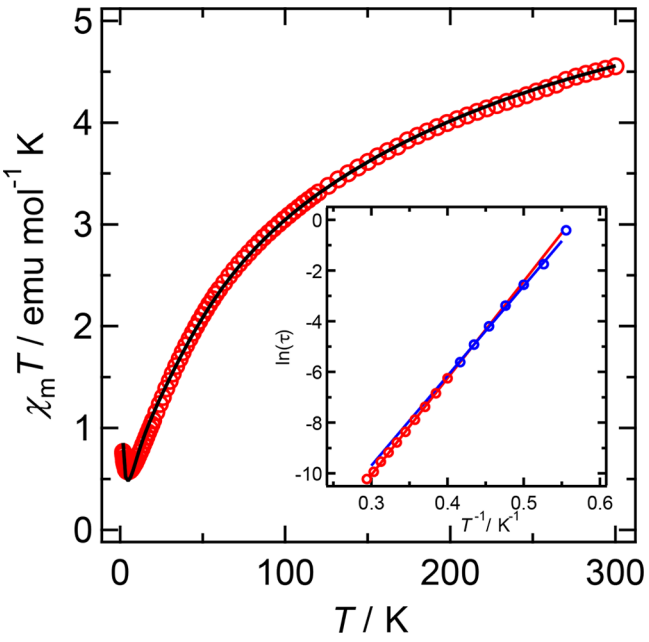

Figure 2. $\chi_m T$ versus T plot for **2** (red) and calculated fitting (black). The fittings are calculated from the values described in the text. Inset: relaxation time (τ) versus $1/T$ plot for **2**.

the value expected for two uncorrelated Mn^{III} ions and one Cu^{II} ion (6.375 emu mol^{-1} K, g = 2.00). The $\chi_m T$ value gradually decreases as the temperature is lowered, reaching a minimum value of 0.57 emu mol^{-1} K at 4.5 K, before rapidly increasing as the temperature is lowered to 1.0 K and then decreasing rapidly below 1.0 K. Magnetic susceptibility data in the higher-temperature region suggest the occurrence of intratrimer antiferromagnetic interactions, while the low-temperature increase in the $\chi_m T$ value indicates the occurrence of intrachain ferromagnetic interactions. The sudden decrease below 1.0 K is likely to result from the magnetic anisotropy of the system. The magnetic susceptibility data were analyzed using an isosceles triangle model with the following Heisenberg spin Hamiltonian:

$$\hat{H} = -2J_{CuMn}(2S_{Cu}\cdot S_{Mn}) - 2J_{MnMn}(S_{Mn}\cdot S_{Mn})$$

Intertrimer magnetic interactions were included as mean-field approximations (zJ'), where z is the number of neighboring molecules and J' represents the intertrimer exchange coupling constant. Least-squares calculations using the data collected above 1.1 K yielded the best-fit values J_{MnMn} = −11.6(1) cm^{-1}, J_{CuMn} = −31.1(6) cm^{-1}, and zJ' = +1.55(2) cm^{-1} with g_{Mn} = 1.96 and g_{Cu} = 2.07. The trimer units, each with an $S = {}^1/_2$ spin ground state due to the intratrimer antiferromagnetic interactions, stack to form a ferromagnetic helix. Note that the Cu^{II} ion in **2** has an unpaired spin in a $d_{x^2-y^2}$ orbital and the Mn^{III} ion in the next trimer unit polarizes its spin onto the occupied d_{z^2} orbital of the Cu^{II} ion. This accidental orthogonality of the magnetic orbitals leads to the occurrence of intrahelix ferromagnetic interactions.

Alternating-current (ac) magnetic susceptibility measurements were performed on a powder sample of **2** in the temperature range 1.8−3.5 K, and the results are shown in Figure 3. Both in-phase and out-of-phase signals show frequency

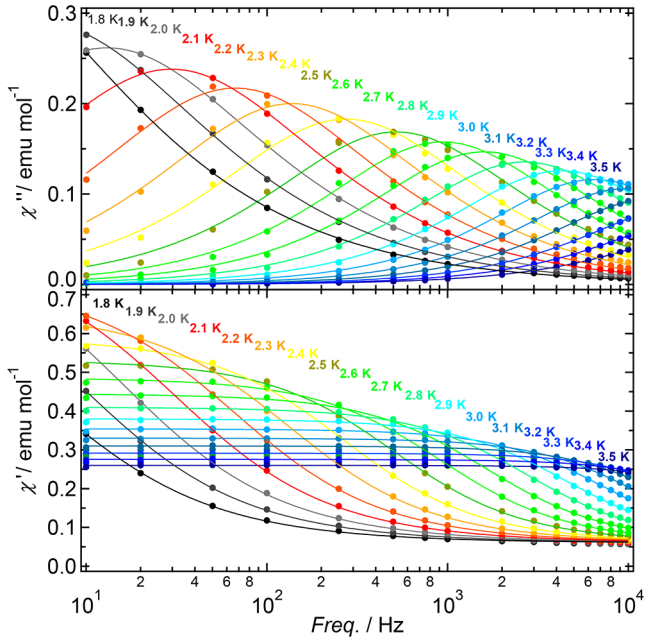

Figure 3. Frequency dependence of the ac magnetic susceptibility for **2**.

dependence, and their peak maxima move to the lower-temperature region as the ac frequency is lowered, suggesting that **2** is either a SMM or a SCM. The magnetic relaxation of transition-metal-based SMMs and SCMs obeys the Arrhenius law, and the Arrhenius plot using the relaxation times (τ) approximated by fitting the ac response using the Debye model clearly shows two distinct lines in the high- and low-temperature regions, with a crossover temperature of 2.4 K (Figure 2, inset). Least-squares calculations for the Arrhenius equation gave the best-fit parameters of $\tau_{0,high} = 4.5 \times 10^{-10}$ s and ΔE_{high} = 38.18 K and of $\tau_{0,low} = 1.5 \times 10^{-9}$ s and ΔE_{low} = 35.44 K for the high- and low-temperature regions, respectively. Considering the magnitude of the τ_0 values of previously reported SCM systems,[5] the τ_0 values obtained in the high-temperature region suggest that **2** is a SCM, an assignment further supported by the observation of a hysteresis loop under a coercive field of 400 Oe at 450 mK (Figure S1 in the Supporting Information, SI).

Monodispersibility of the magnetic relaxation for **2** was confirmed by Cole−Cole plots (Figure 4), which give α values of 0.14 and 0.39 at 3.5 and 1.8 K, respectively (full-fitting parameters are provided in Table S1 in the SI). The high-temperature value indicates a narrow distribution of relaxation times.[14] In this system, there are two relaxation processes. The present compound is slightly effluorescent, meaning that the two observed relaxation processes may originate from the existence of structurally defective chains, a result of lattice solvent loss and the finite-chain effect.[15]

Previous theoretical studies on SCM systems with narrow domain walls have shown that the energy gap $\Delta\xi$ should correspond to the difference between the activation energies in the high- and low-temperature regions.[5] In the present case, the theoretical value is calculated as $\Delta E_{high} - \Delta E_{low}$ = 38.18 − 35.44 = 2.74 K, which is not consistent with magnetic analysis based on

dx.doi.org/10.1021/ic5002418 | Inorg. Chem. 2014, 53, 4272−4274

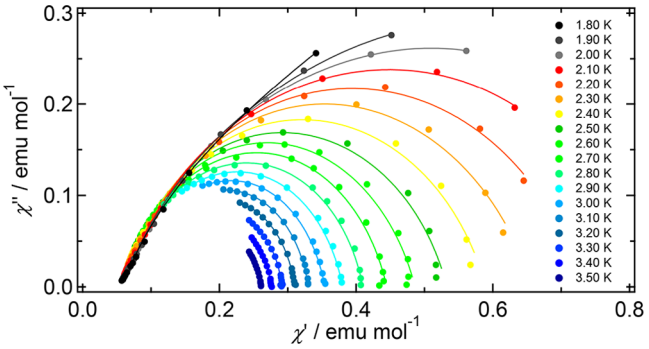

Figure 4. Cole−Cole plots for **2**. The solid lines indicate the theoretical curves calculated using the Debye model.

a trinuclear spin model using the mean-field approximation. In order to elucidate in detail the origins of the two relaxation processes, high-frequency electron paramagnetic resonance measurements and careful consideration of desolvation effects are needed. In addition, further studies including determination of the magnetic anisotropy and magnetic dynamics under a direct-current field are required.

In summary, a heterometallic chiral SCM was synthesized by the metal substitution reaction between $[Mn_3]$ and $[Cu(acac)_2]$ complexes. Cryomagnetic studies reveal that intratriangle magnetic interactions are antiferromagnetic and intertriangle interactions are ferromagnetic. The ferrimagnetic chain exhibits SCM-type character.

■ ASSOCIATED CONTENT

Supporting Information

X-ray crystallographic data in CIF format, experimental procedures and supplementary magnetic data plots. This material is available free of charge via the Internet at http://pubs.acs.org.

■ AUTHOR INFORMATION

Corresponding Authors

*E-mail: ebrechin@staffmail.ed.ac.uk.
*E-mail: oshio@chem.tsukuba.ac.jp.

Notes

The authors declare no competing financial interest.

■ ACKNOWLEDGMENTS

H.O. gratefully acknowledges a Grant-in-Aid for Scientific Research and for Priority Area "Coordination Programming" (area 2107) from MEXT of Japan and a Grant-in-Aid for Scientific Research (Grant 25248014) from the Japan Society for the Promotion of Science. E.K.B. thanks the EPSRC.

■ REFERENCES

(1) (a) Xia, Q.-H; Ge, H.-Q; Ye, C.-P; Liu, Z.-M; Su, K.-X. *Chem. Rev.* **2005**, *105*, 1603−1662. (b) Koeckelberghs, G.; Samyn, C.; Miura, A.; De Feyter, S.; De Schryver, F. C.; Sioncke, S.; Verbiest, T.; De Schaetzen, G.; Persoons, A. *Adv. Mater.* **2005**, *17*, 708−712. (c) Lemieux, R. P. *Acc. Chem. Res.* **2001**, *34*, 845−853. (d) Eerenstein, W.; Mathur, N. D.; Scott, J. F. *Nature* **2006**, *442*, 759−765.

(2) Rikken, G. L. J. A.; Raupach, E. *Nature* **1997**, *390*, 493−494.

(3) (a) Inoue, K.; Kikuchi, K.; Ohba, M.; Ōkawa, H. *Angew. Chem., Int. Ed.* **2003**, *42*, 4810−4813. (b) Imai, H.; Inoue, K.; Kikuchi, K.; Yoshida, Y.; Ito, M.; Sunahara, T.; Onaka, S. *Angew. Chem., Int. Ed.* **2004**, *42*, 5618−5621. (c) Coronado, E.; Gómez-García, C. J.; Nuez, A.; Romero, F. M.; Waerenborgh, J. C. *Chem. Mater.* **2006**, *18*, 2670−2681. (d) Kaneko, W.; Kitagawa, S.; Ohba, M. *J. Am. Chem. Soc.* **2007**, *129*, 248−249. (e) Decurtins, S.; Schmalle, H. W.; Scneuwly, P.; Oswald, H. R. *Inorg. Chem.* **1993**, *32*, 1888−1892. (f) Coronado, E.; Galán-Mascarós, J. R.; Gómez-García, C. J.; Martínez-Agudo, J. M. *Inorg. Chem.* **2001**, *40*, 113−120.

(4) (a) Aromí, G.; Aubin, S. M. J.; Bolcar, M. A.; Christou, G.; Eppley, H. J.; Folting, K.; Hendrickson, D. N.; Huffman, J. C.; Squire, R. C.; Tsai, H.-L.; Wang, S.; Wemple, M. W. *Polyhedron* **1998**, *17*, 3005−3020. (b) Gatteschi, D.; Sessoli, R. *Angew. Chem., Int. Ed.* **2003**, *42*, 268−297. (c) Oshio, H.; Nakano, M. *Chem.—Eur. J.* **2005**, *11*, 5178−5158. (d) Oshio, H.; Hoshino, N.; Ito, T.; Nakano, M. *J. Am. Chem. Soc.* **2004**, *126*, 8805−8812.

(5) Coulon, C.; Miyasaka, H.; Clérac, R. *Struct. Bonding (Berlin)* **2006**, *122*, 163−206.

(6) Bai, Y.-L.; Tao, J.; Wernsdorfer, W.; Sato, O.; Huang, R.-B.; Zheng, L.-S. *J. Am. Chem. Soc.* **2006**, *128*, 16428−16429.

(7) Cavigli, L.; Sessoli, R.; Gurioli, M.; Bogani, L. *Phys. Status Solidi A* **2006**, *203*, 1402−1408.

(8) (a) Oshio, H.; Nihei, M.; Yoshida, A.; Nojiri, H.; Nakano, M.; Yamaguchi, A.; Karaki, Y.; Ishimoto, H. *Chem.—Eur. J.* **2005**, *11*, 843−849. (b) Oshio, H.; Nihei, M.; Koizumi, S.; Shiga, T.; Nojiri, H.; Nakano, M.; Shirakawa, N.; Akatsu, M. *J. Am. Chem. Soc.* **2005**, *127*, 4568−4569.

(9) Inglis, R.; Milios, C. J.; Jones, L. F.; Piligkos, S.; Brechin, E. K. *Chem. Commun.* **2012**, *48*, 181−190.

(10) A SMM of $[Mn^{III}_6O_2(O_2CMe)_2(sao)_6(EtOH)_4]$ (**3**), which has a dimeric form of a trinuclear complex, has a energy barrier of $\Delta E = 28$ K and $\tau_0 = 3.6 \times 10^{-8}$ s. Milios, C. J.; Raptopoulou, C. P.; Terzis, A.; Lloret, F.; Vicente, R.; Perlepes, S. P.; Escuer, A. *Angew. Chem., Int. Ed.* **2004**, *43*, 210−212.

(11) Jones, M. M. *J. Am. Chem. Soc.* **1959**, *81*, 3188−3189.

(12) Crystal structure data for **2**: $C_{27}H_{30}N_3Cl_3CuMn_2O_{10}$, 836.31 g mol^{-1}, hexagonal $P6_5$, a = 17.5632(17) Å, c = 18.423(3) Å, V = 4921.4(12) Å^3, Z = 6, T = 200 K, final R1 = 0.057, wR2 = 0.088 [$I > 2\sigma(I)$], Flack parameter = 0.10(3). The intensity data were recorded on a Bruker SMART Apex CCD system with Mo Kα radiation (λ = 0.71073 Å). The structure was solved by direct methods and refined by full-matrix least-square techniques on F^2 using *SHELXTL*. CCDC 984121 contains the supplementary crystallographic data for this paper. The data can be obtained free of charge from The Cambridge Crystallographic Data Centre via www.ccdc.cam.ac.uk/data_request/cif.

(13) BVS calculations yielded values of 2.23, 3.45, and 3.29 for Cu1, Mn1, and Mn2, respectively, assuming Cu^{II} and Mn^{III}.

(14) Cole, K. S.; Cole, R. H. *J. Chem. Phys.* **1941**, *9*, 341−352.

(15) (a) Coulon, C.; Clérac, R.; Lecren, L.; Wernsdorfer, W.; Miyasaka, H. *Phys. Rev. B* **2004**, *69*, 132408. (b) Zhen, Y.-Z.; Tong, M.-L.; Zhang, W.-X.; Chen, X.-M. *Angew. Chem., Int. Ed.* **2006**, *45*, 6310−6314. (c) Bernot, K.; Bogani, L.; Caneschi, A.; Gatteschi, D.; Sessoli, R. *J. Am. Chem. Soc.* **2006**, *128*, 7947−7956.